PROCEEDINGS OF SCIENCE

Towards mixed QCD×EW corrections to the charged-current Drell-Yan process with leptonic decay at high transverse masses

Christian Biello,[a] **Amlan Chakraborty,**[b] **Giulio Gambuti,**[a] **Raoul Röntsch**[b,c] **and Chiara Signorile-Signorile**[d,*]

[a] *Institute for Theoretical Physics, ETH Zürich, Wolfgang-Pauli-Str. 27, 8093 Zürich*
[b] *Tif Lab, Dipartimento di Fisica, Universitá di Milano, Via Celoria 16, I-20133 Milano, Italy*
[c] *INFN, Sezione di Milano, Via Celoria 16, I-20133 Milano, Italy*
[d] *Theoretical Physics Department, CERN, 1211 Geneva 23, Switzerland*
E-mail: cbiello@phys.ethz.ch, amlan.chakraborty@unimi.it, ggambuti@phys.ethz.ch, raoul.rontsch@unimi.it, chiara.signorile-signorile@cern.ch

The Drell–Yan process is a key precision benchmark at the Large Hadron Collider and a sensitive probe of SM and SMEFT effects. Fully exploiting future LHC data requires percent-level SM predictions, motivating precise EW and mixed QCD×EW corrections. In this proceeding we report of the progress towards the calculation of mixed QCD×EW corrections to charged-current Drell-Yan with leptonic decay at high transverse masses, performed within the Nested Soft-Collinear Subtraction framework. After presenting a validation at NLO, we show results for the NNLO real corrections and compare their impact in the neutral-current and newly developed charged-current channels. These contributions are essential to match the current and future precision of LHC measurements, especially in regions where electroweak effects are enhanced by Sudakov logarithms.

CERN-TH-2026-149
TIF-UNIMI-2026-8

Loops and Legs in Quantum Field Theory (LL2026)
12-17, April, 2026
Bayreuth, Germany

*Speaker

© Copyright owned by the author(s) under the terms of the Creative Commons Attribution-NonCommercial-NoDerivatives 4.0 International License (CC BY-NC-ND 4.0) All rights for text and data mining, AI training, and similar technologies for commercial purposes, are reserved. ISSN 1824-8039 . Published by SISSA Medialab.

PoS(LL2026)049

1. Introduction

The Drell–Yan process is one of the most important reactions at hadron colliders, providing a clean probe of the Standard Model and playing a central role in precision measurements and searches for new physics. In particular, charged-current Drell–Yan (CCDY) production, involving a W boson decaying leptonically, is a cornerstone of the LHC electroweak physics program. As the LHC enters the precision era, with experimental uncertainties reaching the percent level, increasingly accurate theoretical predictions are required. While NLO QCD and electroweak (EW) corrections and NNLO QCD calculations are well established for DY-like processes, mixed QCD×EW corrections are becoming essential to match the experimental precision.

This report presents the first steps toward the computation of mixed QCD×EW corrections to the CCDY process, focusing on the high-transverse-mass region. In this regime, electroweak Sudakov logarithms enhance the virtual corrections [1, 2], leading to sizeable effects in the tails of differential distributions.

2. Set up of the calculation

We focus on the LO process $pp \to \ell^{\pm}\nu$ and write schematically the perturbative expansion of the partonic cross section as

$$\hat{\sigma} = \hat{\sigma}^{\mathrm{LO}} \left(1 + \alpha_s\, \delta\sigma_{\mathrm{qcd}}^{\mathrm{NLO}} + \alpha_{\mathrm{ew}}\, \delta\sigma_{\mathrm{ew}}^{\mathrm{NLO}} + \alpha_s^2\, \delta\sigma_{\mathrm{qcd}}^{\mathrm{NNLO}} + \alpha_s\alpha_{\mathrm{ew}}\, \delta\sigma_{\mathrm{mix}}^{\mathrm{NNLO}} + \dots\right) \tag{1}$$

where α_s and α_{ew} are the strong and electroweak coupling constants respectively. From a power-counting perspective, NLO QCD corrections are typically the dominant effect, while NLO electroweak and NNLO QCD contributions are at the percent level. Although mixed QCD×EW corrections are formally suppressed, electroweak Sudakov logarithms can enhance them significantly in high-energy regions, making them relevant for precision predictions.

The computation of mixed QCD×EW corrections faces two main challenges: the evaluation of two-loop amplitudes and the treatment of real radiation. The virtual contributions involve multi-scale two-loop Feynman integrals, which have been addressed through both analytic and semi-analytic approaches (see for instance Ref. [3–5] for neutral-current calculations, and Ref. [6] for charged current results). Real radiation contributions generate infrared singularities from soft and collinear emissions, which are handled using the nested soft-collinear subtraction (NSC) method [7]. Its extension to mixed corrections must consistently account for both gluon and photon radiation.

3. NLO Electroweak Corrections and validation against `POWHEG`

As a first step, the NLO QCD and the NLO electroweak corrections have been computed within the NSC framework. These corrections provide a useful benchmark and allow for a detailed study of the structure of the calculation. At the integrated level, the NLO electroweak corrections to the CC-DY process amount to approximately -3% of the leading-order cross section. However, their impact is significantly larger at the differential level. In particular, in the transverse mass range between 200 and 800 GeV, the corrections can reach values of order 10%, reflecting the presence

PoS(LL2026)049

of Sudakov logarithms. To validate the calculation, we developed an independent implementation in the POWHEG framework [8]. The comparison shows excellent agreement and provides strong evidence for the correctness of the subtraction procedure and the numerical implementation. In Fig. 1 we present a selection of the observable investigated for the W^+-mediated di-lepton process at NLO EW: the transverse mass m_{T}, the reconstructed invariant mass $m_{e^+\nu_e}$, and the positron transverse momentum p_{T,e^+}. In all observables, the NLO EW corrections reduce the LO prediction over the entire kinematic range. Their magnitude increases with the characteristic energy scale of the process, reaching approximately 10%–13% in the highest bins considered. This behaviour is consistent with the expected enhancement of negative electroweak Sudakov logarithms at large momentum transfers. The differences between the results obtained within the NSC and PWG frameworks remain at the sub-percent level throughout the studied phase space, confirming the consistency of the two implementations. The lower ratio panels further illustrate the impact of the finite-virtual contribution $H^{(1)}$ in the minimal-subtraction scheme: when this term is omitted, the resulting prediction differs from the full NLO EW result by up to about 10%, demonstrating that $H^{(1)}$ provides a sizeable and non-negligible contribution to the electroweak corrections across the considered kinematic range.

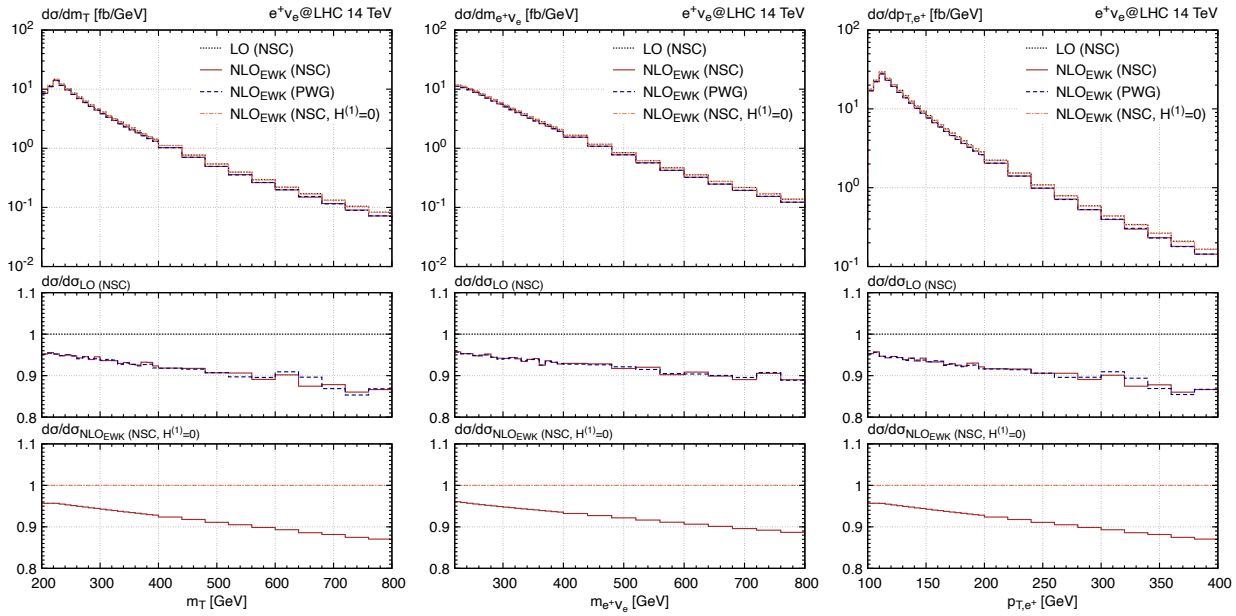

Figure 1: Differential distributions for charged-current Drell–Yan production, $pp \to e^+\nu_e + X$, at the LHC with $\sqrt{s} = 14$ TeV. The upper panels show the m_{T}, $m_{e^+\nu_e}$, and p_{T,e^+} spectra at LO and NLO EW accuracy. The middle panels display the ratios to the LO prediction, while the lower panels compare the full NLO EW result with the approximation obtained by setting $H^{(1)} = 0$. Results from the NSC and POWHEG (PWG) implementations are shown for comparison. See the text for details.

PoS(LL2026)049

4. Organisation of the results for mixed corrections at NNLO

After the subtraction of infrared singularities, the remaining finite contributions can be organized into different components corresponding to double-virtual, real-virtual, and double-real contributions. These are further decomposed into fully-resolved (FR), single-unresolved (SU), and double-unresolved (DU) contributions, which we specify below. In terms of these three contributions the result reads

$$2s_{ab}\,\mathrm{d}\hat{\sigma}_{ab}^{\mathrm{NNLO}} = 2s_{ab}\left[\mathrm{d}\hat{\sigma}_{ab}^{\mathrm{FR}} + \mathrm{d}\hat{\sigma}_{ab}^{\mathrm{SU}} + \mathrm{d}\hat{\sigma}_{ab}^{\mathrm{DU}}\right]. \tag{2}$$

The fully resolved contributions correspond to four-body kinematics and are evaluated numerically. The phase space is divided into sectors, each treated independently, allowing for efficient parallelization. In each sector, only a limited number of kinematic configurations need to be considered, simplifying the numerical integration. The resulting expressions are fully differential and locally finite, leading to stable numerical evaluations. Although the analytic expressions can be quite involved in a general reference frame, they simplify considerably in the partonic centre-of-mass frame, where compact structures emerge. For the sake of illustration, we focus on the partonic channel $q(p_1) + \bar{q}'(p_2) \to \ell(p_3) + \bar{\ell}'(p_4)(+g(p_5) + \gamma(p_6))$, define the Born-level configuration as $\mathcal{H} = 1_q, 2_{\bar{q}'}, 3_\ell, 4_{\bar{\ell}'}$. The fully-resolved contribution that can be directly implemented in four dimensions in a Monte Carlo framework reads [1]

$$\mathrm{d}\hat{\sigma}_{q\bar{q}'}^{\mathrm{FR}} = \left\langle (I - S_g)(I - S_\gamma)\,\Omega_1^{q\bar{q}'}\,F_{\mathrm{LM}}(\mathcal{H}|5_g, 6_\gamma)\right\rangle, \tag{3}$$

with

$$\begin{aligned}\Omega_1^{q\bar{q}'} = &\sum_{i=1,2}(1 - C_{g\gamma,i})\left[(1 - C_{gi})\,\omega^{\gamma i,gi}\,\theta_a^{(i)} + (1 - C_{\gamma i})\,\omega^{\gamma i,gi}\,\theta_c^{(i)}\right] \\ &+ \sum_{\substack{i,j=1,2\\ i\neq j}}(1 - C_{gj})(1 - C_{\gamma i})\,\omega^{\gamma i,gj} + \sum_{i=3,4}\sum_{j=1,2}(1 - C_{gj})(1 - C_{\gamma i})\left[\omega^{\gamma i,gj} + \omega^{\gamma i,gj}\right].\end{aligned} \tag{4}$$

In the equation above, S_i represent the single soft operator that extract the leading behaviour in the $E_i \to 0$ limit. C_{kl} (related to the $p_k \parallel p_l$ limit) and $C_{kl,i}$ (related to the $p_k \parallel p_l \parallel p_i$ limit) identifies the double and triple collinear operator, respectively. The $\omega^{\gamma i,gi}$ and $\omega^{\gamma i,gj}$ are the triple-collinear and double-collinear partition functions, which each isolate a well-defined subset of collinear singularities. Triple-collinear partitions further require the introduction of sectors ($1 = \theta^{(a)} + \theta^{(c)}$) to disentangle strongly-ordered configurations. Upon fixing the unresolved partons to be $5_g, 6_\gamma$, only two distinct sectors are required to implement the fully-resolved contributions for each of the 2 triple-collinear partitions, namely $\theta^{(\alpha)}\omega^{\gamma i,gi} \equiv \theta^{(\alpha)}\omega^{gi,\gamma i} = \{\theta^{(a)}\,\omega^{51,61}, \theta^{(a)}\,\omega^{52,62}, \theta^{(c)}\,\omega^{51,61}, \theta^{(c)}\,\omega^{52,62}\}$. The double-collinear sectors required for this calculation are selected by the functions $\omega^{51,62}$, $\omega^{51,63}$, $\omega^{51,64}$, $\omega^{52,61}$, $\omega^{52,63}$, $\omega^{52,64}$. We note that each sector can be parameterized and run independently [2]. In Sec. 5 we present the numerical impact of the various sectors and partitions, and compare the results with the NCDY predictions.

[1] Notation and conventions are the same as in Ref. [10] and [11].

[2] In the rest of the manuscript we will refer to the sectors as (5161a, 5161c, 5262a, 5262c, 5162, 5163, 5164, 5261, 5263, 5264).

PoS(LL2026)049

Next, we consider the single-unresolved contribution, which can be decomposed into terms with boosted and un-boosted kinematics. The subset of the former involving only the first initial state reads

$$\begin{aligned} \mathrm{d}\hat{\sigma}^{\mathrm{SU,\,sb,\,1}}_{q\bar{q}'} = [\alpha_{\mathrm{ew}}] \left\langle Q_q^2\, O^g_{\mathrm{nlo}} \left[\tilde{P}^{\mathrm{NLO}}_{qq}(E_c, z) + \tilde{\omega}^{\gamma 1, g1}_{\gamma \| 1}\, \log \eta_{15}\, \bar{P}^{\mathrm{AP},0}_{qq,R}(z) \right] \otimes F_{\mathrm{LM}}(\mathcal{H}|5_g) \right\rangle \\ + [\alpha_s] \left\langle C_{\mathrm{F}}\, O^{\gamma}_{\mathrm{nlo}} \left[\tilde{P}^{\mathrm{NLO}}_{qq}(z) + \tilde{\omega}^{\gamma 1, g1}_{g \| 1}\, \log \eta_{15}\, \bar{P}^{\mathrm{AP},0}_{qq,R}(z) \right] \otimes F_{\mathrm{LM}}(\mathcal{H}|5_\gamma) \right\rangle , \end{aligned} \tag{5}$$

where the $O^{\alpha}_{\mathrm{nlo}}$ is the fully resolved operator defined as $O^{\alpha}_{\mathrm{nlo}} = (1 - S_\alpha)(1 - \sum_i C_{\alpha i})$. The functions $\tilde{P}^{\mathrm{NLO}}_{qq}(z, E)$ and $\bar{P}^{\mathrm{AP},0}_{qq,R}(z)$ are related to the tree-level splitting functions [3] and the symbol $\otimes$ indicate the convolutions of such splitting functions with the matrix elements where the incoming momentum p_1 is rescaled by a the energy fraction factor z. Next, the $\tilde{\omega}^{\gamma 1, g1}_{\alpha \| 1}$ indicates the result of applying the limit $\alpha \parallel 1$ onto the partition function $\omega^{\gamma 1, g1}$. Finally we have $\eta_{ab} = (1 - \cos\theta_{ab})/2$, with θ_{ab} being the angle between the directions of partons a and b. The elastic (un-boosted) component of the SU contribution is given by

$$\begin{aligned} \mathrm{d}\hat{\sigma}^{\mathrm{SU,\,el}}_{q\bar{q}'} = \left\langle O^g_{\mathrm{nlo}}\, F^{(\mathrm{EW})}_{\mathrm{RV,fin}}(\mathcal{H}|5_g) \right\rangle + \left\langle O^{\gamma}_{\mathrm{nlo}}\, F^{(\mathrm{QCD})}_{\mathrm{RV,\,fin}}(\mathcal{H}|5_\gamma) \right\rangle \\ + [\alpha_{\mathrm{ew}}] \left\langle O^g_{\mathrm{nlo}} \left[\mathcal{G}^{(\mathrm{EW})}_{\mathrm{nlo}} F_{\mathrm{LM}}(\mathcal{H}|5_g) \right] \right\rangle + [\alpha_{\mathrm{s}}] \left\langle O^{\gamma}_{\mathrm{nlo}} \left[C_{\mathrm{F}}\, \mathcal{G}^{(\mathrm{QCD})}_{\mathrm{nlo}} F_{\mathrm{LM}}(\mathcal{H}|5_\gamma) \right] \right\rangle , \end{aligned} \tag{6}$$

where in the first line we have introduced the finite remainder of the real-virtual corrections, $F^{(\mathrm{EW})}_{\mathrm{RV,fin}}$ ($F^{(\mathrm{QCD})}_{\mathrm{RV,\,fin}}$), involving one EW (QCD) virtual exchange and one QCD (EW) emission. In the second line, we have introduced the functions

$$\mathcal{G}^{(\mathrm{QCD})}_{\mathrm{nlo}} = \frac{2\pi^2}{3} + 6L_c + 3\log\eta_{12} + 2\mathrm{Li}_2(1 - \eta_{12}) \tag{7}$$

$$\mathcal{G}^{(\mathrm{EW})}_{\mathrm{nlo}} = Q_\ell^2\, A_\ell + Q_\ell Q_q\, A_{\ell q}(\eta_{13}) + Q_\ell Q_{\bar{q}'}\, A_{\ell q}(\eta_{23}) + Q_q Q_{\bar{q}'}\, A_{qq}(\eta_{12}) \tag{8}$$

which involve the logarithmic term $L_c = \log(2E_c/\mu)$ where E_c is the partonic center-of-mass energy. The coefficient functions A are simple combinations of constants, L_c, $L_\ell = \log(2E_\ell/\mu)$, $\log(\eta)$, where E_ℓ is the energy of the charged lepton, and $\mathrm{Li}_2(1 - \eta)$. In the next section we present results for a selection of the contributions mentioned above, emphasising the differences with respect to the NCDY production.

5. Selection of contributions and comparison with neutral-current Drell-Yan

Double unresolved corrections. We then turn to discussing the implementation of the fully resolved contribution, focusing on the fully resolved component. We present the comparison of the equivalent correction for both NCDY and CCDY to emphasise some relevant differences and similarities. Table 1 reports the integrated contributions of representative double-real subtraction sectors for both NCDY and CCDY (W^+). In agreement with the expectations from the singularity structure of the subtraction framework, sectors naturally group into pairs with nearly identical integrated cross sections. This pairing is particularly evident for the $(5161a, 5262a)$, $(5161c, 5262c)$, $(5163, 5263)$, $(5164, 5264)$ and $(5162, 5261)$ sectors, whose results agree within the numerical

[3] The explicit definition can be found in Eq. (2.66) in Ref. [10]

PoS(LL2026)049

Double-real sectors contributions: NCDY vs CCDY (W^+) (100 seeds, $5.0\times10^6\times15\ +\ 5.0\times10^7\times10$)			
NCDY		CCDY (W^+)	
Sector	*Cross-section* [fb]	*Sector*	*Cross-section* [fb]
5161a	0.93220 ± 0.00011	5161a	0.17887 ± 0.00009
5262a	0.93222 ± 0.00011	5262a	0.17873 ± 0.00009
5161c	0.04374 ± 0.00030	5161c	0.04200 ± 0.00017
5262c	0.04356 ± 0.00031	5262c	0.04227 ± 0.00017
5163	0.08572 ± 0.00024	5163	0.05167 ± 0.00005
5263	0.08647 ± 0.00025	5263	0.05177 ± 0.00005
5164	0.12337 ± 0.00036	5164	0.12578 ± 0.00038
5264	0.12344 ± 0.00036	5264	0.12549 ± 0.00038
5162	0.36610 ± 0.00023	5162	0.22284 ± 0.00013
5261	0.36571 ± 0.00020	5261	0.22296 ± 0.00013

Table 1: Comparison of representative double-real subtraction sectors in NCDY and CCDY (W^+). The close agreement within the pairs $(5161a, 5262a)$, $(5161c, 5262c)$, $(5163, 5263)$, $(5164, 5264)$, and $(5162, 5261)$ reflects the sector symmetries discussed in the text. The results are produced by combining 100 independent seeds, each obtained with 15 integration iterations to pre-sample the phase space with 5×10^6 points, and then 10 iterations with 5×10^7 points.

integration uncertainties. The existence of these sector pairs reflects the fact that they are associated with analogous singular limits. While this pattern is present in both neutral- and charged-current Drell–Yan production, the hierarchy among sector pairs differs significantly. In NCDY, the contributions are strongly ordered, with some pairs suppressed by more than an order of magnitude relative to the dominant ones. In CCDY, the spread is considerably reduced, resulting in a more uniform distribution of the integrated cross section across the different singular configurations.

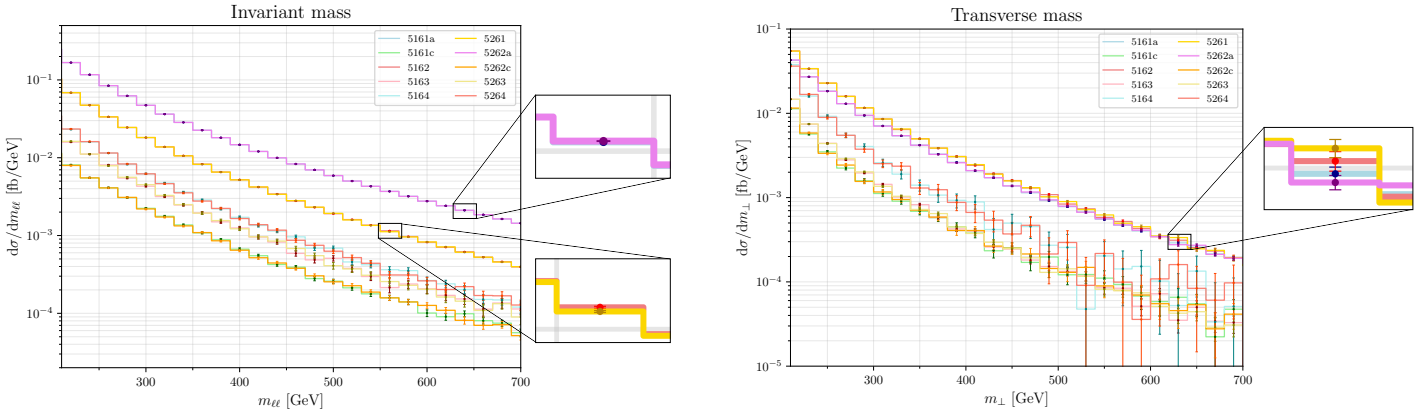

Figure 2: Comparison of the contribution of different double-real sectors to a given distribution: dilepton-invariant mass distribution for the neutral-current Drell–Yan process (left), and W-boson transverse mass distribution for the charged-current Drell–Yan process (right).

Figure 2 presents the sector decomposition of the finite double-real contribution at differential

PoS(LL2026)049

level. The patterns largely mirror those observed for the integrated cross section, but are more pronounced in the distributions. In NCDY, the sectors form nearly degenerate pairs across the full kinematic range, while in CCDY this structure is broken, leading to a more homogeneous distribution among sectors. The different relative importance of triple- and double-collinear sectors further highlights the distinct singularity structure of the two processes.

Single unresolved corrections. As shown in Table 2, the CC process displays a less symmetric sector structure than NCDY, already at the single-unresolved level, leading to a different hierarchy among the dominant contributions. Figure 3 compares representative single-unresolved contributions in neutral- and charged-current production. While the NC sectors exhibit a nearly symmetric behaviour, reflecting the underlying process symmetries, the CC channel shows sizeable asymmetries between analogous sectors due to the charged lepton–neutrino final state and the different partonic flavour structure. In addition, the EW contributions are significantly reduced in magnitude in CCDY, leading to smaller cancellations among sectors. These features illustrate how the singularity structure and sector hierarchy become more process dependent in the CC case.

$\mathcal{O}_{\text{nlo}}$ **contributions: NCDY vs CCDY** (W^+) (100 seeds, $5.0 \times 10^5 \times 15 \; + \; 5.0 \times 10^6 \times 10$)			
NCDY		CCDY (W^+)	
Contribution	*Cross-section* [fb]	*Contribution*	*Cross-section* [fb]
oqcd	-0.27737 ± 0.00029	oqcd	0.20859 ± 0.00008
oewk_fs_53	-7.56029 ± 0.00214	oewk_fs_53	-1.32523 ± 0.00015
oewk_fs_54	-7.61950 ± 0.00252	oewk_fs_54	-4.04229 ± 0.00139
oewk_is	-8.21967 ± 0.00069	oewk_is	-0.77722 ± 0.00019
rvqcd_is	3.18048 ± 0.00015	rvqcd_is	0.72593 ± 0.00016

Table 2: Comparison of SU contributions between NCDY and CCDY (W^+). The results are produced by combining 100 independent seeds, each obtained with 15 integration iterations to pre-sample the phase space with 5×10^5 points, and then 10 iterations with 5×10^6 points.

6. Outlook and Conclusions

The computation of mixed QCD×EW corrections to the charged-current Drell–Yan process represents a significant step toward achieving the level of precision required for current and future collider experiments. The results obtained so far demonstrate that these corrections, although formally subleading, play an important role in precision phenomenology, especially in the high-energy regime. Looking ahead, further developments are expected in several directions. These include the completion of the full NNLO calculation and improvements in numerical efficiency. Moreover, the possibility of deriving mixed corrections for arbitrary hadronic scattering through the abelianization of QCD results offers an intriguing avenue for future research.

PoS(LL2026)049

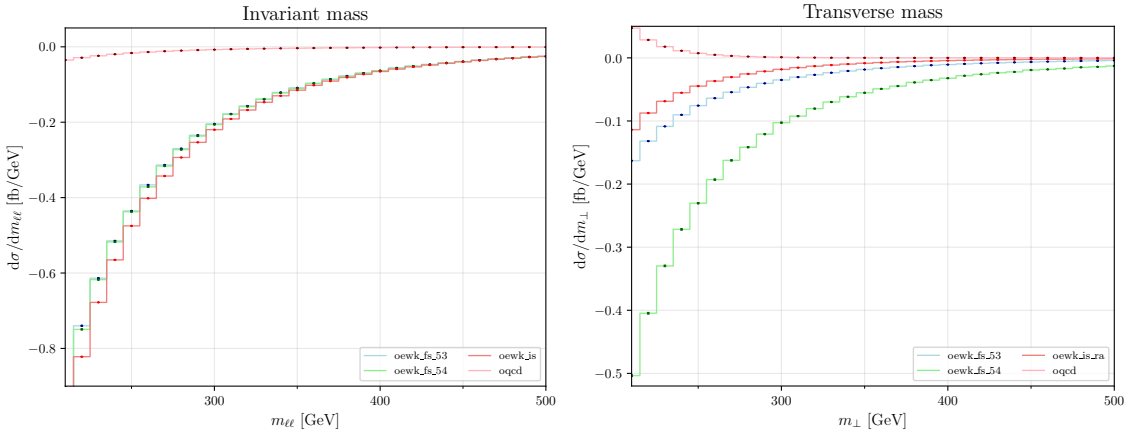

Figure 3: Comparison of the contribution of different double-real sectors for neutral-current (top) and charged-current (bottom) Drell-Yan production.

Acknowledgments

C.B. acknowledges funding from the Swiss National Science Foundation, grant 10001706. C.B. and C.S-S. wish to thank the Physics Department of the University of Milan for hospitality during work on this project. The work of R.R. and A.C. is supported by the Italian Ministry of Universities and Research (MUR) through grant PRIN2022BCXSW9.

References

[1] J. H. Kuhn, A. A. Penin and V. A. Smirnov, *Summing up subleading Sudakov logarithms*, Eur. Phys. J. C 17 (2000), 97-105.

[2] A. Denner and S. Pozzorini, *One loop leading logarithms in electroweak radiative corrections. 2. Factorization of collinear singularities*, Eur. Phys. J. C 21 (2001), 63-79.

[3] H. Matthias, A. von Manteuffel and R. M. Schabinger, *Multiple polylogarithms with algebraic arguments and the two-loop EW-QCD Drell-Yan master integrals*, Phys. Rev. D, 102 (2020)

[4] M. Heller, A. von Manteuffel, R. M. Schabinger and H. Spiesberger, *Mixed EW-QCD two-loop amplitudes for $q\bar{q} \to \ell^+\ell^-$ and γ_5 scheme independence of multi-loop corrections*, JHEP 05 (2021), 213

[5] T. Armadillo, R. Bonciani, S. Devoto, N. Rana and A. Vicini, *Two-loop mixed QCD-EW corrections to neutral current Drell-Yan*, JHEP 05 (2022), 072

[6] T. Armadillo, R. Bonciani, S. Devoto, N. Rana and A. Vicini, *Two-loop mixed QCD-EW corrections to charged current Drell-Yan*, JHEP 07 (2024), 265

[7] F. Caola, K. Melnikov, and R. Röntsch, *Nested soft-collinear subtractions in NNLO QCD computations*, *Eur. Phys. J.* C77 (2017), no. 4, 248.

[8] T. Ježo and P. Nason, *On the Treatment of Resonances in Next-to-Leading Order Calculations Matched to a Parton Shower*, JHEP 12 (2015), 065.

PoS(LL2026)049

[9] S. Frixione, Z. Kunszt, and A. Signer, *Three jet cross-sections to next-to-leading order*, *Nucl. Phys.* B467 (1996) 399–442.

[10] F. Buccioni, F. Caola, H. A. Chawdhry, F. Devoto, M. Heller, A. von Manteuffel, K. Melnikov, R. Röntsch and C. Signorile-Signorile, *Mixed QCD-electroweak corrections to dilepton production at the LHC in the high invariant mass region*, JHEP 06 (2022), 022.

[11] F. Devoto, K. Melnikov, R. Röntsch, C. Signorile-Signorile, D. M. Tagliabue and M. Tresoldi, *Integrated subtraction terms and finite remainders for arbitrary processes with massless partons at colliders in the nested soft-collinear subtraction scheme*, JHEP 01 (2026), 137.

[12] F. Devoto, K. Melnikov, R. Röntsch, C. Signorile-Signorile and D. M. Tagliabue, *A fresh look at the nested soft-collinear subtraction scheme: NNLO QCD corrections to N-gluon final states in $q\overline{q}$ annihilation*, JHEP 02, 016 (2024).

[13] F. Devoto, K. Melnikov, R. Röntsch, C. Signorile-Signorile, D. M. Tagliabue and M. Tresoldi, *Towards a general subtraction formula for NNLO QCD corrections to processes at hadron colliders: final states with quarks and gluons*, JHEP 08, 122 (2025).

[14] C. Biello, A. Chakraborty, G. Gambuti, R. Röntsch, C. Signorile-Signorile, *in preparation*.

PoS(LL2026)049